

UNIVERSIDADE FEDERAL DA PARAÍBA
CENTRO DE CIÊNCIAS DA SAÚDE
PROGRAMA DE PÓS-GRADUAÇÃO EM ODONTOLOGIA

**SÍNTESE, CARACTERIZAÇÃO, CITOTOXICIDADE E
IMUNOMODULAÇÃO DE VIDROS BIOATIVOS
DOPADOS COM PRATA EM LEUCÓCITOS
HUMANOS**

Jefferson Muniz de Lima

SAPIENTIA AEDIFICAT

2016

JEFFERSON MUNIZ DE LIMA

**SÍNTESE, CARACTERIZAÇÃO, CITOTOXICIDADE E
IMUNOMODULAÇÃO DE VIDROS BIOATIVOS DOPADOS COM
PRATA EM LEUCÓCITOS HUMANOS**

Dissertação apresentada ao Programa de Pós-Graduação em Odontologia, da Universidade Federal da Paraíba, como parte dos requisitos para obtenção do título de Mestre em Odontologia – Área de Concentração em Odontologia.

Orientador: Prof. Dr. Lúcio Roberto Cançado Castellano

Co-Orientador: Prof. Dr. Paulo Rogério Ferreti Bonan

João Pessoa

2016

Catálogo na publicação
Seção de Catalogação e Classificação

L732s Lima, Jefferson Muniz de.

Síntese, caracterização, citotoxicidade e imunomodulação de vidros bioativos dopados com prata em leucócitos humanos / Jefferson Muniz de Lima. - João Pessoa, 2016.

30 f. : il.

Orientação: Lúcio Roberto Cançado Castellano.

Coorientação: Paulo Rogério Ferreti Bonan.

Dissertação (Mestrado) - UFPB/CCS.

1. Odontologia. 2. Imunomodulação. 3. Leucócitos. I. Castellano, Lúcio Roberto Cançado. II. Bonan, Paulo Rogério Ferreti. III. Título.

UFPB/BC



ATA DA DEFESA PÚBLICA DE DISSERTAÇÃO DE MESTRADO
DEFESA DE Nº:

Aos dezoito dias do mês de dezembro do ano de 2016, às 14:00 horas, no Auditório da Pós-Graduação em Odontologia/UFPB, reuniram-se os membros da banca examinadora composta pelos professores doutores Lúcio Roberto Cançado Castellano (Orientador e Presidente), Eliton Souto De Medeiros (membro vinculado ao Programa de Pós-graduação em Odontologia – UFPB) e a Profa. Dra. Fabia Danielle Sales Cunha Medeiros E Silva (membro externo) a fim de arguirm o mestrando Jefferson Muniz de Lima, com relação ao seu trabalho final de curso de mestrado (dissertação), sob o título "Síntese, Caracterização, Citotoxicidade e Imunomodulação de Vidros Bioativos Dopados com Prata em Leucócitos Humanos". Aberta a sessão pelo presidente da mesma, coube a candidata, na forma regimental, expor o tema de sua dissertação, dentro do tempo regulamentar. Em seguida, foi questionado pelos membros da banca examinadora, sendo as explicações necessárias fornecidas e as modificações solicitadas registradas. Logo após, os membros da banca examinadora reuniram-se em sessão secreta, tendo chegado ao seguinte julgamento, que, de público, foi anunciado: 1º Examinador (membro externo): Conceito "Aprovado"; 2º Examinador (membro vinculado ao PPGO): Conceito "Aprovado"; e 3º Examinador (Orientador e Presidente): Conceito "Aprovado". O que resultou em conceito final igual: "APROVADO", o que permite a candidata fazer jus ao título de Mestre em Odontologia. Os documentos utilizados para avaliação do candidato durante o processo aqui descrito apresentam-se como prova documental do mesmo e, como tal, serão anexadas a esta ata para arquivamento. Nada mais havendo a tratar, foi lavrada a presente ata, que será por mim assinada, Raíssa Karen Gomes dos Santos, secretária do Programa de Pós-graduação em Odontologia da UFPB, pela presidente, pelos demais membros da banca, e pelo candidato.

Secretária

1º Examinador – Membro Externo

2º Examinador – Membro do PPGO

3º Examinador – Presidente

Candidato

Confere com o Original

Jacqueline Santos Aureliano Alves
Secretária da Pós-Graduação em
Odontologia / UFPB
Mat. SIAPE 11834591

NOTAS PRELIMINARES

A presente Dissertação foi redigida conforme o Manual para Normatização da Defesa do Trabalho Final proposto pelo Programa de Pós-Graduação em Odontologia da Universidade Federal da Paraíba, adotando o formato alternativo. Um artigo científico compõe este trabalho de Dissertação, o qual foi redigido de acordo com as exigências da revista na qual foi submetido (Frontiers in Immunology).

DEDICATÓRIA

Aos voluntários que gentilmente consentiram doar sangue.

AGRADECIMENTOS

Aos meus pais, José Alves e Valdenira Muniz, por todo amor, carinho, incentivos e perseverança. Se hoje cheguei aqui, o mérito é de vocês;

Às minhas irmãs, Valéria e Thayná, que sempre me amaram e ajudaram em todos os momentos;

À toda família Muniz e Alves por sempre acreditarem em meu potencial, em especial a Vó Alzenir por ser uma segunda mãe;

À Lanne, verdadeira companheira de pesquisa, por estar ao meu lado nessa caminhada;

Ao meu primo Edu que tanto conviveu comigo durante a pós graduação;

Aos professores Lúcio Castellano e Paulo Bonan, exemplos ímpares de orientadores, por terem apostado e acreditado em meu potencial, pela disponibilidade, pelos ensinamentos, condução e acolhida nessa fase. Torso para que minha jornada permaneça sob seus cuidados.

À Roberta Bonan pelo suporte laboratorial e pelo fornecimento das amostras;

Ao professor Eliton Medeiros por elucidações no campo da engenharia e pelo suporte técnico;

À professora Joelma Souza pela companhia e por sempre barganhar um material ou outro;

À Luana, Panmella e aos professores Ronaldo Sarmiento e Ana Carolina pelo auxílio na rotina do laboratório;

À Professora Fábria por aceitar compor a banca avaliadora e pelas contribuições com este trabalho;

Aos funcionários da Escola Técnica de Saúde pelo suporte de infraestrutura;

Aos demais professores do PPGO-UFPB e aos órgãos de fomento à pesquisa;

À Rebeca Tibau e Roberta pelo suporte nas atividades do laboratório;

Aos demais companheiros de turma pela parceria nesses dois anos;

Aos grandes amigos Ana Dal Piva, Suzana, Filype, Igor e Melk pelos momentos de risadas ou tretas e pela feroz torcida em momentos de luta. Que o vento esteja sempre ao nosso favor, mas, do contrário, saberei onde encontrar alicerce.

RESUMO

O vidro bioativo (BG) possui aplicações no campo da engenharia tecidual, como o preenchimento para regeneração óssea, estimulante da regeneração e revestimento de implantes. O BG pode ser conjugado à prata (Ag), o que pode lhe conferir propriedades antimicrobianas. Considerando que a atividade imunomoduladora do BG associado a prata (BGAg) não tenha sido avaliada, o objetivo deste trabalho foi avaliar a citotoxicidade e atividade imunomoduladora do BG e do BGAg. Amostras pertencentes ao sistema $58\text{SiO}_2 \cdot (36-x)\text{CaO} \cdot 6\text{P}_2\text{O}_5 \cdot x\text{Ag}_2\text{O}$, onde $x = 0$ ou 1 mol%, respectivamente, foram sintetizadas pelo método sol-gel, e caracterizadas por Microscopia Eletrônica de Varredura (SEM), Microscopia de Força Atômica (AFM), Análise Termogravimétrica (TGA), Difração de raios X (XRD) e Espectroscopia Raman Amplificada por Superfície (Raman-SERS). A citotoxicidade foi avaliada em monócitos (PBMCs) e polimorfonucleares (PMNs) humanos de sangue periférico. A caracterização microscópica mostrou partículas ≤ 74 μm com aspecto irregular e superfície porosa. As análises RAMAN-SERS confirmaram a inclusão de prata nas micropartículas de sílica. A viabilidade dos PBMCs na presença do BG e do BGAg mostrou-se ser dependente da dose. As amostras do BGAg apresentaram maior toxicidade ($\text{LC}_{50} = 0,005\%$) quando comparadas com as amostras do BG ($\text{LC}_{50} = 0,106\%$). Os vidros bioativos não alteraram o perfil basal de liberação de citocinas e espécies reativas de oxigênio (ROS), embora as amostras BG tenham sido capazes de reduzir os níveis de ROS induzidos por zymozan. Portanto, as partículas de vidro bioativo dopado com prata não difere na morfologia ou propriedades físicas, apesar de que a incorporação dessa modificação ter aumentado a citotoxicidade desse material, com potencial imunomodulador de resposta imune inata.

Palavras-chave: Vidro bioativo 58S, Imunomodulação, Leucócitos

ABSTRACT

Bioactive glasses (BG) has application in tissue engineering for bone regeneration, coating for implants and stimulatory of wound healing. BG can be conjugated to antimicrobial ions like silver (Ag) giving it antibacterial activity. Once the immunomodulatory activity of bioactive glasses doped with silver was not investigated before, the aim of this work was to evaluate the cytotoxic and immunomodulatory effect of BG and silver-doped bioactive silica (BGAg). BG and BGAg samples belonging to the system $58\text{SiO}_2 \cdot (36-x)\text{CaO} \cdot 6\text{P}_2\text{O}_5 \cdot x\text{Ag}_2\text{O}$, where $x = 0$ and 1 mol%, respectively, were synthesized via sol-gel method, and characterized by Scanning Electron Microscopy (SEM), Atomic Force Microscopy (AFM), Surface-enhanced Raman Spectroscopy (Raman-SERS), Differential Thermal Analysis (DTA), Thermal Gravimetric Analysis (TGA) and X-ray diffraction (XRD). Cytotoxicity, cytokine modulation and oxidative stress were performed in human peripheral blood mononuclear cells (PBMCs) and polymorphonuclear neutrophils (PMNs) cultures. Microscopy characterization showed particles $\leq 74 \mu\text{m}$ with irregular and porous surface. RAMAN-SERS analyses confirmed silver inclusion within BGAg samples. PBMC viability in presence of BG or BGAg was dose-dependent. Samples of the BGAg presented high toxicity ($\text{LC}_{50} = 0.005\%$) relative to BG ($\text{LC}_{50} = 0.106\%$) against PBMCs. The glasses did not changed cytokines and Reactive oxygen species (ROS) basal secretion profiles. Therefore, BG samples decrease ROS's levels when coincubated with positive control. Overall, Ag-modified glass particles had impact on the morphology or physical properties, although ion incorporation has increased its cytotoxicity.

Keywords: bioactive glass 58S, Immunomodulation, Leukocytes

LISTA DE ABREVIATURAS E SIGLAS

AFM - Atomic force microscopy
Ag⁺ - Ionic silver
BG-Bioactive Glass
BGAg - Silver doped bioactive glass
CI - Confidence interval
CaO - Calcium oxide
DTA - Differential thermal analysis
DRX - X-Ray Diffraction
FBS - Fetal bovine serum
FI - Fluorescent Intensity
H₂O - dihydrogen monóxide
HIV - Human immunodeficiency virus
HCV - Hepatitis C virus
HBV - Hepatitis B virus
IL - Interleukin
IFN γ - Interferon-gama
LC - Lethal concentration
mL- Mililiter
Na₂O - Sodium oxide
Nm - Nanometer
pH - Hydrogenionic potential
P₂O₅ - Phosphorus pentoxide
PBMC - Peripheral blood mononuclear cell
RAMAN-SERS - Surface-enhanced Raman spectroscopy
Ra - Average roughness
Rq - Root mean square roughness
Rp - Maximum profile peak height
Rv - Maximum profile valley depth

Rz - Ten-points mean height roughness

RLU - Relative luciferase units

ROS - Reactive oxygen species

M - Molar

mg - Milligram

mM - Millimolar

PenStrep - Penicillin and streptomycin

PHA - Phytohemagglutinin

PMN - Polymorphonuclear neutrophil

SEM - Scanning electron microscope

SiO₂ - Silicon dioxide

SEM - Scanning Electron Microscopy

TCP - Tricalcium phosphate

TEOS - Tetraethylorthosilicate

TEP - Triethyl phosphate

TGA - Thermal Gravimetric Analysis

TGFβ1 - Transforming growth factor beta 1

TNF-α - Tumor necrosis factor alpha

VEGF - Vascular endothelial growth factor

wt/vl - weight/volume

°C - Celsius

μg - Microgram

μm - Micrometer

μl - Microliter

SUMÁRIO

1. INTRODUÇÃO	1
2. CAPÍTULO 1	5
INTRODUCTION	6
EXPERIMENTAL	7
BG synthesis	7
BG characterization	7
Samples	8
Assay and data acquisition	9
Statistical Analysis	10
RESULTS AND DISCUSSION	11
Characterization of BG	11
Cell viability in presence of BG and BGAg	15
Oxidative stress	18
Cytokine modulation	19
Conclusions	21
References	23
3. CONSIDERAÇÕES GERAIS	26
4. CONCLUSÃO	27
5. REFERÊNCIAS	28

1. INTRODUÇÃO

O vidro bioativo (Bioactive Glass - BG), descrito inicialmente por Hench, é composto principalmente por dióxido de silício (SiO_2), óxido de cálcio (CaO), pentóxido de fósforo (P_2O_5) e óxido de sódio (Na_2O) [1]. A sua estrutura consiste em uma rede de SiO_2 , tendo o P_2O_5 como coadjuvante e o CaO e o Na_2O como modificadores [2]. O BG tem como principal método de produção o processamento Sol-Gel que consiste na hidrólise do tetraetilortossilicato, $\text{Si}(\text{OC}_2\text{H}_5)_4$ em meio ácido, produzindo SiO_2 na forma semelhante ao vidro [3]. A bioatividade desse material concedeu sua aplicação no campo da regeneração e engenharia tecidual [2,4].

Dentre as aplicações bem estabelecidas do BG na odontologia, pode-se citar o uso como: enxertos para preenchimento de espaços corpóreos [5], revestimento para implantes ósseos [6,7] arcabouço para reparo tecidual, com arranjo poroso semelhante ao trabeculado ósseo [4].

Materiais bioativos, como o BG, podem desenvolver no osso ligações químicas capazes de permitir a integração do biomaterial à área receptora [6]. Pesquisas apontam para propriedades biológicas também em tecidos moles. Ostomel et al. [8] observaram uma diminuição do tempo de coagulação sanguínea induzida por microesferas porosas de BG. Esse material também pode ter atividade na angiogênese, o que é importante para a cicatrização de feridas [9]. A indução do reparo tecidual pelo BG 58S (SGBG-58S), BG em escala nanométrica (NBG-58S) e do derivado do BG 45S5 pode ser constatada no estudo de Lim et al. [10], em que feridas em ratos tratadas com esse material tiveram o tempo de cicatrização reduzido quando comparado ao grupo sem tratamento.

Diante disso, os BGs vivenciaram eras de desenvolvimento bem definidas desde sua descoberta: a era das aplicações clínicas e a era da regeneração tecidual. Atualmente, os BGs experimentam sua era de inovações que inclui a associação com materiais inorgânicos para aplicações além da regeneração óssea [11]. O BG pode ser conjugado à prata (Ag), conferindo-lhe propriedades antimicrobianas, como mostrou o estudo de Day et al. [12] que, utilizando esferas de sílica porosas produzidas em passo único com brometo de cetiltrimetilamônio e

conjugadas ao $\text{Ca}(\text{NO}_3)_2$ e ao AgNO_3 , observaram efeito antimicrobiano sobre *E. coli* e *S. aureus*. Os ensaios de Zhu et al. [13] constataram que o BG poroso 58S (SM58S), preparado a partir da modificação superficial do BG poroso 58S (M58S) pelo silano KH-550 e carregado com Ag^{2+} , também tiveram significativa atividade antibacteriana contra *E. coli* e *S. aureus*. No entanto, o mesmo efeito não foi observado pelo BG com ausência de prata. Outro estudo [25] observou ação inibitória de nanopartículas de vidro bioativo dopadas com prata contra *P. aeruginosa* e *C. albicans*. Tais propriedades podem minimizar complicações em cirurgias de enxertos, como, por exemplo, infecções.

O mecanismo pelo qual o íon prata exerce a sua toxicidade contra células de mamíferos não é bem esclarecido, mas sabe-se que em bactérias, sua atividade antimicrobiana pode estar relacionada com a ligação ao DNA, a interação com componentes celulares e a interferência com o transporte de elétrons, pois reage com carboxilato de proteínas, hidroxilas e tióis [14,15]. A ação de ions Ag^{2+} deriva da sua ligação com proteínas microbianas carregadas negativamente impedindo a sua replicação.

Com a finalidade de mensurar a viabilidade celular, Labbaf et al. [16] encubaram partículas esféricas de vidro bioativo (85mol% SiO_2 e 15mol%CaO) com diâmetro médio de 250nm pela técnica Sol-Gel em culturas de células mesenquimais humanas (hMSCs). A viabilidade celular não foi influenciada no período de 1 a 4 dias após a incubação e não observaram danos ao DNA. As concentrações de 150 e 200 mg/ml, contudo, reduziram significativamente a atividade metabólica das hMSCs após 7 dias de cultivo.

O 45S5 Bioglass® em pequenas concentrações (0,01% wt/vol) provou aumentar a proliferação de fibroblastos de linhagem 208F em um período de 24h. Resultados antagônicos ocorreram quando altas concentrações desse BG foram incubadas com as culturas por até 72h. A secreção do fator de crescimento vascular endotelial (VEGF) foi constatada nas culturas de fibroblastos, exceto naquelas expostas a altas concentrações do BG (0,1–10%), indicando uma relação dependente da dose. Utilizando o mesmo BG em arcabouços de poli(ácido glicólico) observou-se, após implantação subcutânea em ratos, boa

tolerância e neovascularização no interior do BG em um período de 28 e 42 dias [17].

Ainda em relação à mensuração do VEGF, Detsch et al. [18] observaram que fibroblastos humanos da linhagem CD-18CO quando em contato com o BG S53P4 (53% SiO₂, 23% Na₂O, 20% CaO, 4% P₂O₅) com diferentes tamanhos de partículas (0,5-0,8mm, 1,0-2,0mm, e 2,0-3,15mm) e em diferentes concentrações (0-1%), durante 72h, não revelaram citotoxicidade significativa. A secreção do VEGF mostrou-se ser dependente do tamanho da partícula: partículas entre 0,5-0,8 mm e 1,0-2,0 mm estimularam esse fator, já as partículas entre 2,0-3,15 mm causaram inibição.

Day and Boccaccini [19] incubaram culturas de macrófagos derivados de monócitos coletados de sangue humano periférico com BGs e observaram que concentrações acima de 0,01% causaram diminuição da viabilidade celular. Os autores concluíram que os BGs estudados não têm atividade imunomoduladora do TNF- α , IL-6 e IL-10, mas são capazes de controlar a secreção de TNF- α em resposta ao estímulo do LPS. O autor também concluiu que composições químicas diferentes influenciam a modulação da resposta inflamatória.

Apesar do grande potencial de bioatividade dos BGs em diversas áreas da medicina regenerativa [4-8,13,20], há dúvidas acerca da exposição dos BGs a longo prazo aos tecidos vivos, podendo perpetuar reações adversas nos tecidos circundantes à implantação. A citotoxicidade desse material também é pouco explorada, podendo variar com a composição química do BG, em especial quando há presença de prata, já que esse metal possui alta citotoxicidade [12].

Estudos *in vitro* têm larga utilização para determinação da citotoxicidade aguda e imunomodulação causadas por biomateriais. Dentre os tipos celulares utilizados, os PBMCs têm uso recorrente. PBMCs consistem principalmente em linfócitos e monócitos, os quais representam as mais importantes populações de células do sistema imunológico. No sangue, leucócitos representam uma linha celular de defesa hábil em liberar vários mediadores inflamatórios após sua ativação [21].

Respostas imunes mediadas por células são críticas para indução de efeitos indesejados como reações de hipersensibilidade, inflamação crônica e imunoestimulação e a avaliação do perfil de liberação de citocinas é considerada um dos mais importantes indicadores de avaliação dessas respostas deletérias. Os mediadores liberados por células do sistema imunológico também regulam o metabolismo ósseo, podendo gerar reabsorção óssea em torno do implante, levando à rejeição do mesmo [22]. A degradação de biomateriais por fagocitose está relacionada a macrófagos residentes teciduais, bem como seus precursores os monócitos que são uma população constituinte dos PBMCs [24]. Dessa forma, estudos da interface tecido-implante têm demonstrado associação entre macrófagos e áreas de reabsorção óssea [22]. Portanto, para os testes iniciais de biocompatibilidade dos BGs optou-se por utilizar os PBMCs como células teste, uma vez em que eles representam a primeira linha de defesa contra qualquer tipo de implante no corpo humano [23].

As potenciais reações imunológicas moduladas por BG são pouco elucidadas pela literatura, cabendo investigações aprofundadas. Principalmente, devido à larga variação da composição química do biomaterial que, assim como a biocompatibilidade, pode influenciar na resposta imunológica [19]. Desta forma, este trabalho tem o objetivo produzir, caracterizar e avaliar a viabilidade celular e o potencial imunomodulador de vidros bioativos dopados com prata em leucócitos humanos.

2. CAPÍTULO 1

O manuscrito a seguir foi submetido para publicação no periódico *Frontiers in Immunology* e encontra-se em análise.

***Ex vivo* assessment on immunomodulatory effects of bioactive glasses microparticles doped with silver in human leukocytes**

ABSTRACT

Bioactive glasses (BG) has application in tissue engineering for bone regeneration, coating for implants and stimulatory of wound healing. BG can be conjugated to antimicrobial ions like silver (Ag^+) giving it antibacterial activity. Once the immunomodulatory activity of bioactive glasses doped with silver was not investigated before, the aim of this work was to evaluate the cytotoxic and immunomodulatory effect of BG and silver-doped bioactive silica (BGAg). BG and BGAg samples belonging to the system $58\text{SiO}_2 \cdot (36-x)\text{CaO} \cdot 6\text{P}_2\text{O}_5 \cdot x\text{Ag}_2\text{O}$, where $x = 0$ and 1 mol%, respectively, were synthesized via sol-gel method, and characterized by Scanning Electron Microscopy (SEM), Atomic Force Microscopy (AFM), Surface-enhanced Raman Spectroscopy (Raman-SERS), Differential Thermal Analysis (DTA), Thermal Gravimetric Analysis (TGA) and X-ray diffraction (XRD). Cytotoxicity, cytokine modulation and oxidative stress were performed in human peripheral blood mononuclear cells (PBMCs) and polymorphonuclear neutrophils (PMNs) cultures. SEM and AFM images showed particles $\leq 74 \mu\text{m}$ with irregular and porous surface. RAMAN-SERS analyses confirmed silver inclusion within BGAg samples. PBMC viability in presence of BG or BGAg was dose-dependent. Samples of the BGAg presented high toxicity ($\text{LC}_{50} = 0.005\%$) relative to BG ($\text{LC}_{50} = 0.106\%$) against PBMCs. The glasses did not changed cytokines and Reactive oxygen species (ROS) secretion profiles. BG samples decrease ROS's levels when coincubated with positive control. Overall, Ag-modified glass particles had impact on the morphology or physical properties, although ion incorporation has increased its cytotoxicity.

Keywords: bioactive glass 58S, Immunomodulation, Leukocytes

INTRODUCTION

Bioactive glass (BG) consists of a SiO_2 network, having P_2O_5 as an adjuvant and CaO and Na_2O as modifiers [1,2]. The bioactivity of this material allows its application in the field of regeneration and tissue engineering [3]. It can be used in a wide range of applications, such as bioactive fillers in the bone regeneration field [4], coating for implants, dental grafting [5,6] and as scaffold for tissue repair, with porous arrangements similar to trabecular bone [3,7]. BG is most used as hard tissue replacement material, although some studies show remarkable properties in soft tissues repair, as observed in decreased blood coagulation time, angiogenesis and reduced wound healing time [8].

BGs are experiencing innovations such association with inorganic materials such as ions for non-bone therapeutic applications [9]. Silver doped glasses showed antibacterial and antifungal effect against *Escherichia coli*, *Staphylococcus aureus* [10,11], *P. aeruginosa* and *Candida albicans* [12] in comparison to neat BG. Such properties may minimize complications on bone surgery like bacterial infection by topical drug delivering in a controlled and continuous manner [13]. Although, silver loading may increase hypersensitivity, chronic inflammation and immunostimulation due materials exposure [14].

The potential immunomodulatory activity of bioactive glasses has tested before [7,15]. The results indicates differences of immune response modulation depends of composition or particular system from which the bioactive glasses are selected. Some samples indicate potential ability to inhibit the secretion of inflammatory cytokines in the presence of an inflammatory stimulus [15]. However, the immunomodulatory activity of bioactive glasses doped with silver has not been investigated before. There are few studies on the toxicology of Ag^{2+} on normal primary cells of the human immune system on literature. The complete understanding of the specific interactions and dynamic responses of the immune system to different materials is still inconclusive, especially for health applications or safety recommendations [16]. Therefore, the aim of this work was to evaluate the cytotoxic and immunomodulatory effect of BG and silver-doped bioactive silica over human leukocytes.

EXPERIMENTAL

BG synthesis. Samples belonging to the system $58\text{SiO}_2 \cdot (36-x)\text{CaO} \cdot 6\text{P}_2\text{O}_5 \cdot x \text{Ag}_2\text{O}$ with $x = 0$ or 1 mol% (Neat BG, BGA_g) were prepared by sol–gel method (Figure 1). Briefly, hydrolysis and condensation of tetraethyl orthosilicate (TEOS), calcium nitrate tetrahydrate ($\text{Ca}(\text{NO}_3)_2 \cdot 4\text{H}_2\text{O}$), triethyl phosphate (TEP; Sigma Aldrich) and silver nitrate (AgNO_3 ; PlatLab) were used to obtain the gels. The molar ratio of EtOH: TEOS was of 1:1. The other precursors were dissolved in distilled water. The pH of solutions was adjusted to 2 by addition of HNO_3 . The obtained gels were dried for 3 days at room temperature and 2 days in a drying oven, at 120°C . The Neat BG was dried gels were heat treated up to 700°C for 1/2h, at a constant rate of $3^\circ \text{C min}^{-1}$ [19]. Herein, the glasses were passed through a 200-mesh British Standard Sieve (final particles diameter smaller than $74\mu\text{m}$) .

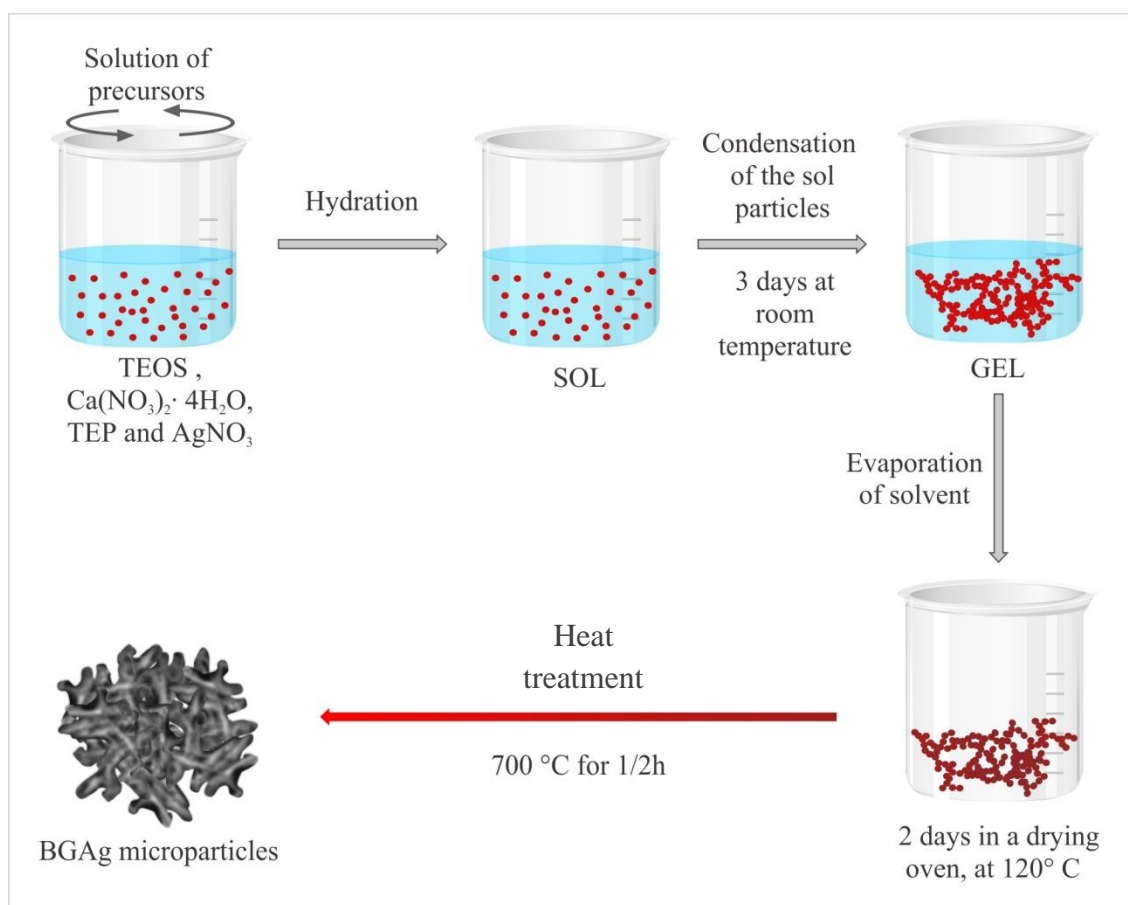


Figure 1. Schematic representation of the sol-gel method for preparation of silver-doped bioglass microparticles.

BG characterization.

Scanning Electron Microscopy (SEM). The morphology of the BG was observed in a Zeiss Quanta 450 (FEITM, FEI Company). 10 μl of 2 mg/ml samples in ethanol were fixed on aluminum stubs and their surfaces covered with gold using a K550X Emitech sputter coater.

Atomic Force Microscopy (AFM). AFM analyses were obtained in a Shimadzu SPM9600 microscopy. One μL of 2 mg/ml in ethanol samples was pipetted onto a mica cover slip, and after 20 minutes imaging was recorded at room temperature (25°C) with the following roughness parameters: average roughness (Ra), root mean square roughness (Rq), maximum profile peak height (Rp), maximum profile valley depth (Rv), and ten-points mean height roughness (Rz).

The X-Ray Diffraction (XRD). spectra was recorded with a Shimadzu XRD-6000 diffractometer, using Cu K α radiation ($\lambda = 1.5418 \text{ \AA}$), with Ni-filter. Specimens were aligned perpendicular to the incident beam and the analysis parameters were step size 0.01° and a diffraction range of 10–90°. The diffractograms were recorded after samples being annealed at 700 °C.

Surface-enhanced Raman Spectroscopy (RAMAN-SERS). For RAMAN-SERS, was employed a QE65000 Spectrometer (Ocean Optics) with a diode laser at 785nm. Analyses were performed at room temperature (25°C) and the Raman spectrum was collected with Ocean Optics data acquisition SpectraSuite spectroscopy software.

Differential Thermal Analysis (DTA) and Thermal Gravimetric Analysis (TGA). Thermal measurements were performed on Shimadzu analyzer DTG-60H, in nitrogen atmosphere, from room temperature to 800 °C, using alumina crucibles, with heating rate of 10 °C/min.

Samples

Materials and methods was structured following the Minimal Information About T cell Assay [17].

Volunteers. This study was approved by local ethics committee. Each of three healthy volunteers signed a written consent to participate according to the Helsinki Declaration of ethical guidelines.

The healthy volunteers were seronegative for HIV and HCV, vaccinated against HBV, had no signs or symptoms of acute infections at the time of blood sampling and PBMC isolation.

Peripheral Blood Mononuclear Cells (PBMC) and Polymorphonuclear neutrophil (PMN) isolation and stimulation. Heparinized whole blood was collected by venipuncture and processed by Histopaque® 1077 and 1119 (Sigma-Aldrich, St. Louis, USA) [18]. The PBMCs and PMNs were washed three times with phosphate buffer and counted using Trypan blue (Sigma-Aldrich, St. Louis, USA) exclusion method in Neubauer chamber with viability $\geq 95\%$. Cells preparations contained $>99\%$ granulocytes as determined by morphological examination of Giemsa-stained cytocentrifuged slides (Shandon, Pittsburgh, PA, USA). Cells were resuspended in equal aliquots of 2×10^6 PBMC/ml and 10^6 PMN/ml in RPMI 1640 medium (Gibco, Life Technologies, UK) supplemented with 10% heat-inactivated fetal bovine serum, 1% PenStrep and 20mM HEPES. All procedures were conducted at room temperature.

Assay and data acquisition

PBMCs viability assay. 100 μ l of PBMC's suspension were stimulated with 5 μ g/ml of phytohemagglutinin (PHA-P; Sigma-Aldrich, St. Louis, USA) and incubated 1:1 with BG (range 1-0.0075% wt/vl) or BGAg (range 1-0.0002% wt/vl) in culture medium in 96 black polystyrene wells flat bottom microplates (Greiner Bio-One, USA) for 24 hours at 37°C in a humidified atmosphere at 5% CO₂.

Cell viability was measured using alamarBlue® according to kit protocol (Bio-Rad, Hercules, EUA). Fluorescence was measured at GloMax®-Multi Microplate Reader (Promega, Madison, USA) and percentage of viability was calculated as follows:

$$\text{Cytotoxicity (\%)} = [(FI\ 590\ \text{of treated samples} / FI\ 590\ \text{of untreated cells}) \times 100]$$

Where: FI 590 = Fluorescent Intensity at 590 nm emission (560 nm excitation)

The lethal concentration 50 (LC50) was determined by semi-log graph plotted with percent of untreated control for each BG and BGAg suspensions.

PMNs viability assay. Cell death was assayed by the LIVE/DEAD™ viability/cytotoxicity kit (Thermo Fisher, Rockford, IL, USA) according to kit

instructions. Briefly, 10^5 PMNs were incubated with BG and BGAg samples for 4 hours at 37°C in a humidified atmosphere at 5% CO₂. Cells were incubated with 80% methanol for death control. 20 min after staining with 1µM calcein and ethidium homodimer, fluorescence visualization was performed using epifluorescent microscope EVOS FL cell imaging system (Life Technologies, Eugene, OR, USA) equipped with a 40x objective, GFP and RFP filter cubes. Quantification of live and dead cells were analyzed in 3 aleatory fields using ImageJ (National Institutes of Health, Bethesda, MD) software according to recommendations [19].

Luminol Enhanced Chemiluminescence Assay. Production of intra and extracellular ROS was analyzed by luminol enhanced chemiluminescence. Briefly, the PMN suspension (2×10^5 cells/ml) were incubated for 45 min at 37 °C and 5% CO₂ with the BG and BGAg samples in white polystyrene 96-wells flat bottom (Greiner Bio-One, USA). Serum-opsonized zymosan (13 mg/ml; Sigma-Aldrich, St. Louis, USA) or medium alone were the positive and negative control, respectively. After incubation, 10^{-4} M luminol (Sigma-Aldrich, St. Louis, USA) was added and chemiluminescence was measured at 2-minute intervals with a luminometer GloMax®-Multi Microplate Reader (Promega, Madison, USA) for a period of 1h at 37°C. Chemiluminescence was expressed as relative light units (RLU) and the area under the curve (AUC) was determined for each stimulus.

Quantification of cytokines release. PBMCs (10^6 cells/ml) were cultured for 24 hours at 48-well plates with the larger subtoxic concentration of BG and BGAg at 37°C in 5% CO₂. PBMCs cultures (with or without 5 µg/ml PHA stimulation) supernatants were analyzed for IL-1β, TNF-α, IL-4, IL-6 and IL-10 by sandwich ELISA assay using OptEIA Kit (Becton Dickinson, Franklin Lakes, New Jersey, USA) according to kit protocol.

Statistical Analysis. Significant differences on cell viability, cytokine production and ROS release between the groups were determined by Kruskal Wallis test with Dunn's post hoc ($\alpha=0.05$) using the software Statistical Package for the Social Sciences version (SPSS) version 2.1 (IBM Corp, New York, EUA).

RESULTS AND DISCUSSION

Characterization of BG

SEM and AFM topographical analyses. The SEM analysis showed irregular and porous surface for all samples (Figure 2). Ethanol evaporation as well as nitrate decomposition during the stabilization process that was carried out to convert the dry gel into glass, can explain the porous nature of BG.

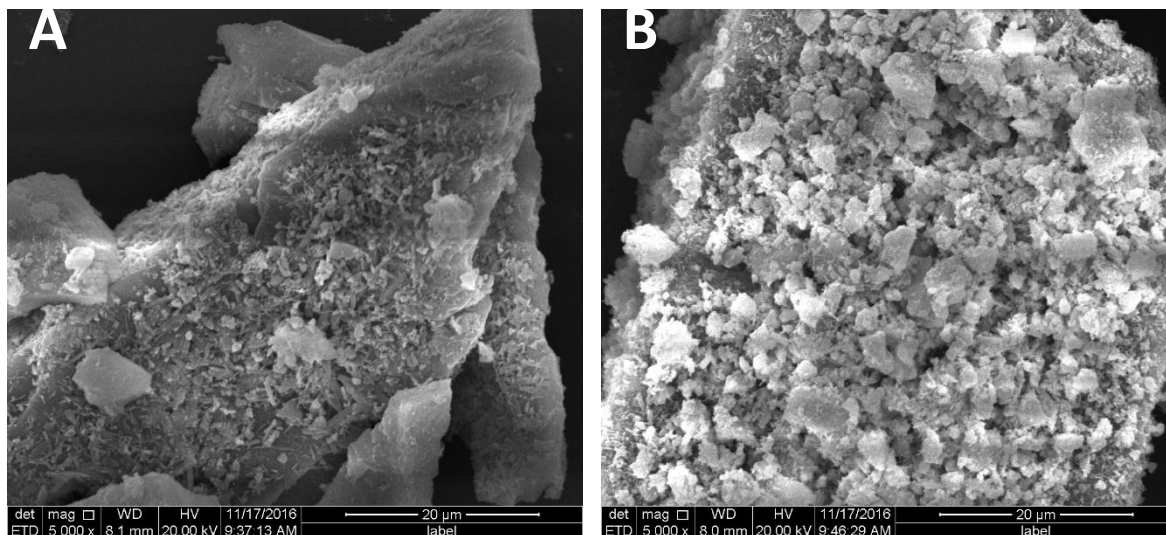
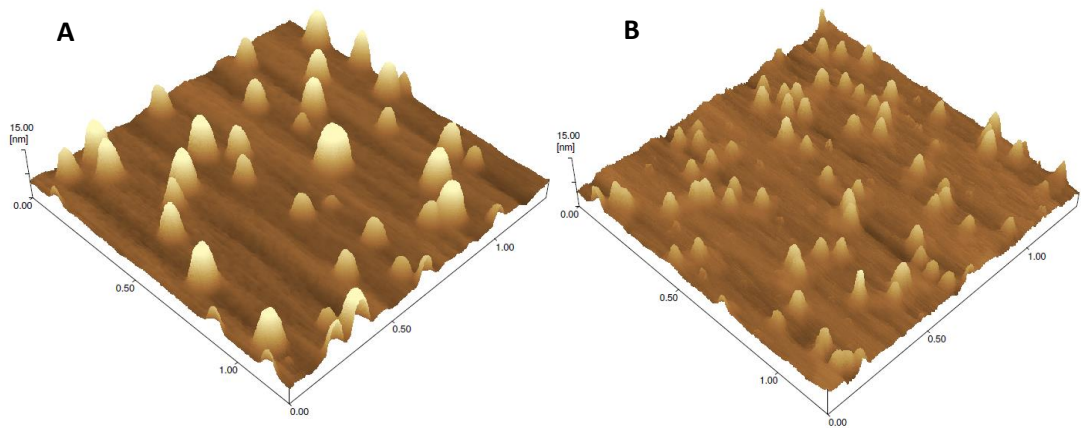


Figure 2. SEM Micrograph of Neat BG (A) and BGAg (B) with 5.000x magnification.

AFM imaging presented in Figure 3 shows the surface roughness analyses (R_a , R_z , R_q , R_p , R_v) of bioglasses. The BG presented a greater roughness surface R_q (Root-mean-square roughness) and R_a (Arithmetic mean roughness) in contrast to BGAg particles. The non-uniform spikes indicate ellipsoidal-like structures. The relative minor roughness of BGAg particles, indicating reduced size, may be explained by the greater density and strength of BGAg due to the Ag distribution, leaving the surface more homogeneous when the solution evaporates and allows the organization of particles on the mica cover slip.



	BG	BGA _g
Ra	1.21	0.70
Rz	14.89	11.29
Rq	2.10	1.15
Rp	12.57	8.71
Rv	2.32	2.58

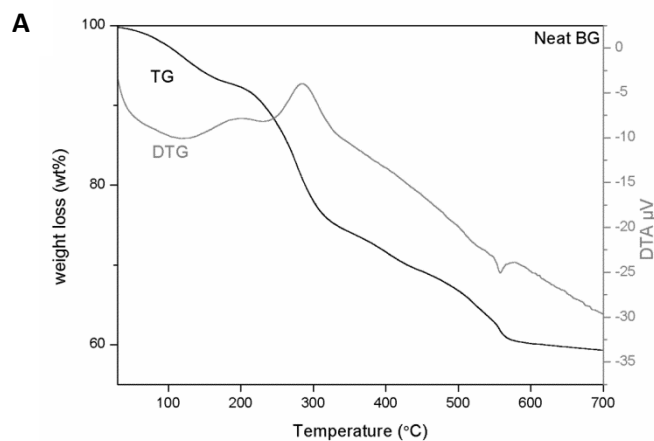
$$Rz = Rp + Rv$$

$$\text{Area} = 1.25 \mu\text{m}^2$$

Figure 3. AFM imaging of BG (A) and BGA_g (B) particles. Values of roughness expressed as mean.

Taken together, the topographical analyses evidence textural properties correlated with *in vitro* increase of hydroxyapatite layer deposition. Such surface may promote intimate contact with the living tissue with niches for cell proliferation [13].

Thermal analysis. DTA and TGA curves for samples Neat BG and BGA_g are shown in Figure 4.



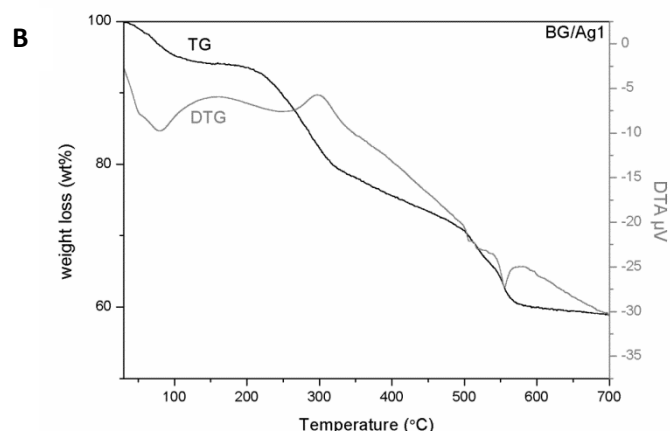


Figure 4. DTA and TGA curves for samples Neat BG (A) and BGAg (B).

For all samples, the first weight loss appeared at the temperature interval between 65°C - 95°C. It is an endothermic peak associated with the elimination of residual alcohol and physisorbed water from the polycondensation reaction that was not removed during drying. The second peak is exothermic, with an onset around 237°C, for all samples, associated with the desorption of chemically adsorbed water or to the removal of organic residues. For the silver-doped samples, an endothermic peak appears around 497°C is attributed to silver oxide decomposition and possibly metallic silver crystals formation. For all samples, a weight loss located around 534°C could be assigned to the decomposition of the unreacted $\text{Ca}(\text{NO}_3)_2$ [20,21]. Taking into account these results, the temperature of 700°C was chosen for the stabilization of all glass powders, since all residues could be removed at temperatures lower than 700°C.

XRD. The XRD results of BG and BGAg samples exhibited mainly amorphous characteristics corresponding to bioactive glass formation (Figure 5). All samples showed incipient crystallization of a tricalcium phosphate (TCP) phase identified as $\text{Ca}_3(\text{PO}_4)_2 \cdot 2\text{H}_2\text{O}$ centered at $2\theta=32^\circ$. This result suggests that the incorporation of silver into the investigated BG samples did not compromise its characteristics that promotes bioactivity [20].

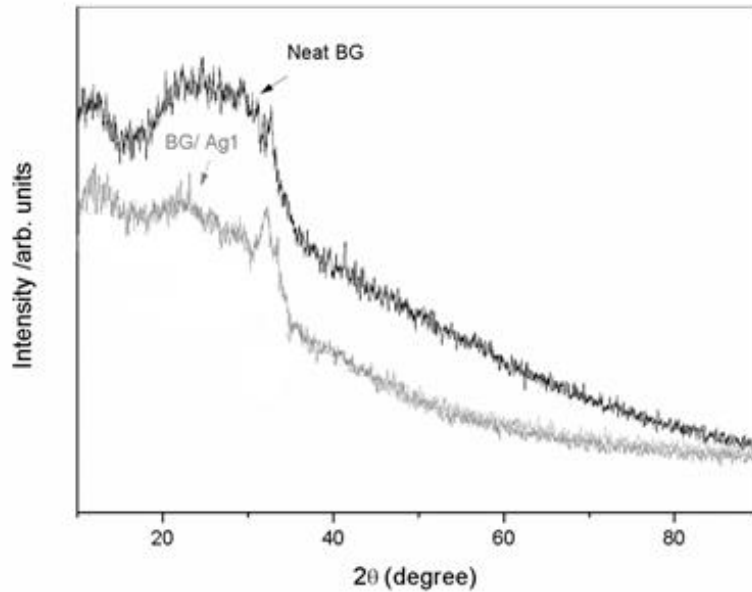


Figure 5. XRD patterns of the $58\text{SiO}_2 \cdot (36-x)\text{CaO} \cdot 4\text{P}_2\text{O}_5 \cdot x\text{Ag}_2\text{O}$ samples.

RAMAN-SERS spectra. The identification and quantification of chemical species by Raman spectroscopy based on vibrational modes were performed to characterize the Ag-doped silica material. Comparing BG and BGAg spectra profile (Figure 6), is perceptible an enhanced Raman signals (red line) of adsorbed molecules. This signal intensification by several orders of magnitude is especially due to the adsorbed species in metal surfaces, a phenomenon named SERS (Surface-Enhanced Raman Scattering) [22,23]. Therefore, the RAMAN-SERS confirmed the Ag signal amplification on silica groups of BGAg samples.

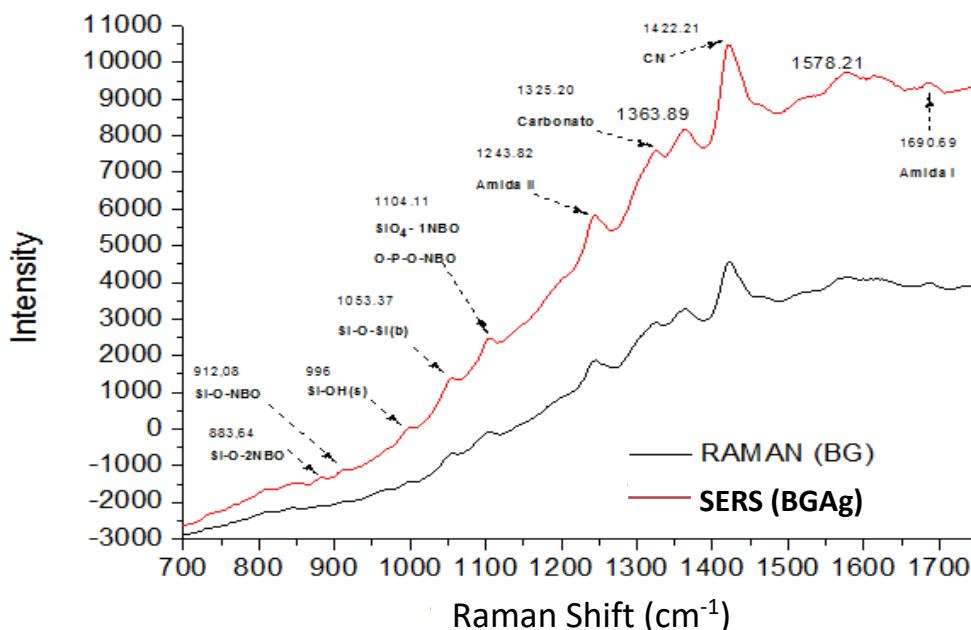


Figure 6. RAMAN-SERS spectra of BG and BGAg samples.

The peak at 1050 cm^{-1} is assigned to the stretching vibration bands associated with Si-O-Si bond in silica tetrahedral form with the different number of non-bridging oxygen (NBO) involving two dimensional structure of $\text{Si}_2\text{O}_5^{2-}$. Generally, vibrations of silica networks are observed between 400 cm^{-1} and 1300 cm^{-1} . A peak observed in the region between 1000 cm^{-1} and 1260 cm^{-1} is attributed to the asymmetric vibration of the Si-O-Si bridging sequence. Raman shifts are more sensitive to the composition changes and the addition of alkali metal ions to the silica network, and peak shifting and intensity variations are usually noticed because of the increase or decrease of the local symmetry of the silica network. The BGAg did not present the expected spectra probably due to the aggregation of metal ions, with uneven distribution when mixed to silica. The lack of uniformity may have reduced the surface area distribution of Ag and compromised proper vibrational profile of the bioglass, without RAMAN-SERS signal [22,23].

Cell viability in presence of BG and BGAg. Cell viability of PBMC was accessed after 24h incubation with BG and BGAg by determining the metabolic capacity of cells to reduce the indicator dye resazurin to fluorescent resorufin. A dose-dependent reduction in cell viability was observed in both samples of BG. The cell viability decreased to values less than 50% of control cells at the highest treatment concentration of 0.125 and 0.0075% for BG and BGAg, respectively. Calculated LC50 values were 0.106% for BG and 0.005% for BGAg.

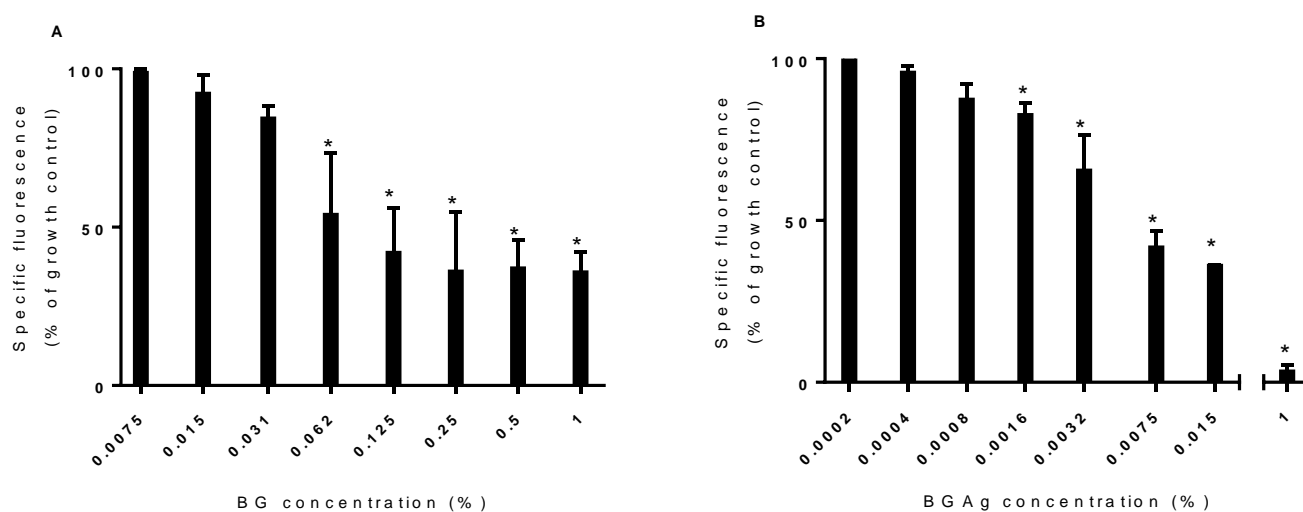


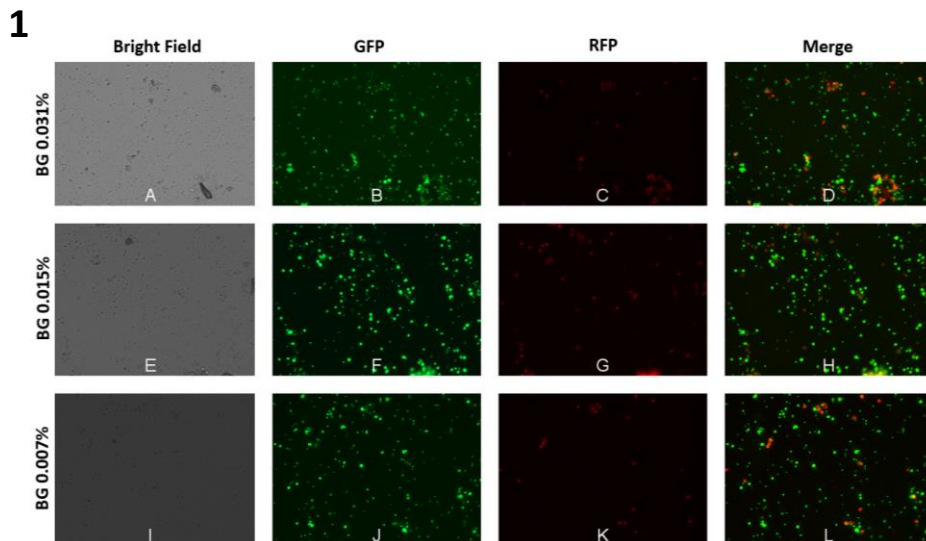
Figure 7. Effect BG (A) and BGAg (B) on PBMC viability. Cell viability after treatment with increasing concentrations BG and BGAg, expressed as percentage of baseline.

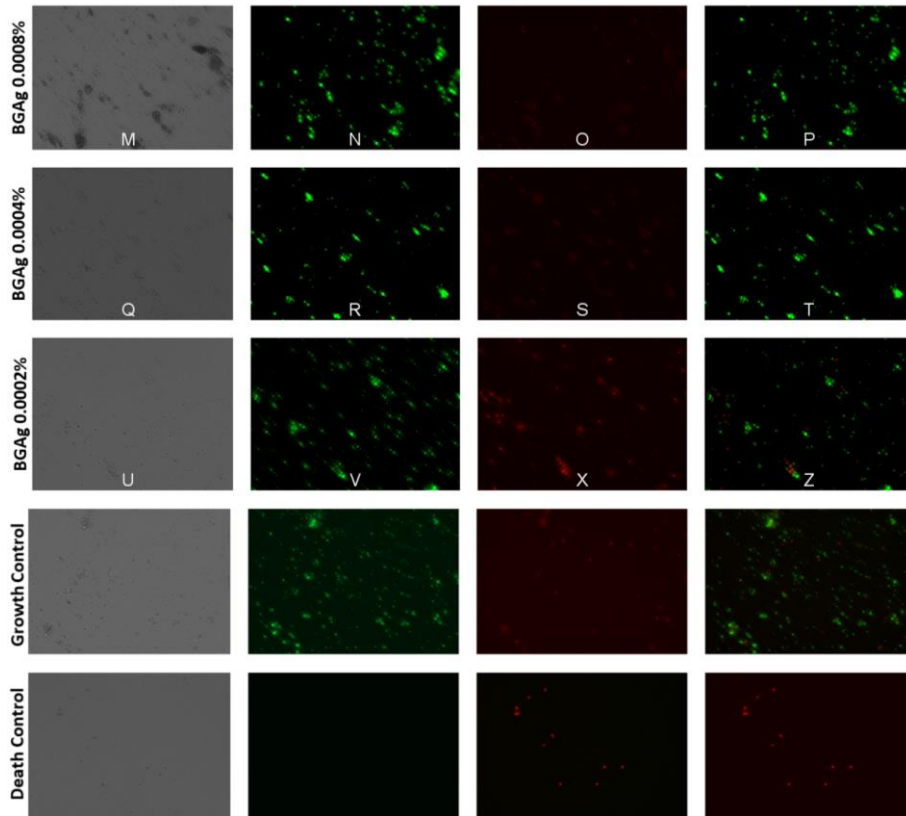
Results shown as median with 95% CI of an experiment performed in triplicate of each volunteer (*P<0.05 compared to growth control).

Over the range of BG concentrations, BG 0.031% was the highest suspension that did not significantly compromised PBMC viability in comparison with growth control. This result is superior than the subtoxic concentration of 0.01% observed in previously work [15].

In addition, there were remarkable differences in cytotoxicity of the Bg and BGAg against PBMCs: the BGAg non-toxic concentration was 0.0008%. Such cytotoxicity might be associated with free Ag²⁺ released in culture medium. Earlier study demonstrated Ag²⁺ cytotoxicity against PBMCs depends on the dose and incubation period [14].

BG and BGAg subtoxic doses in PBMCs populations did not influence the PMN viability according to LIVE/DEAD test. Fluorescence images of PMN cultures stained with ethidium homodimer (damaged cell marker) did not show quantitative differences between samples wells and growth control wells (Figure 8).





2

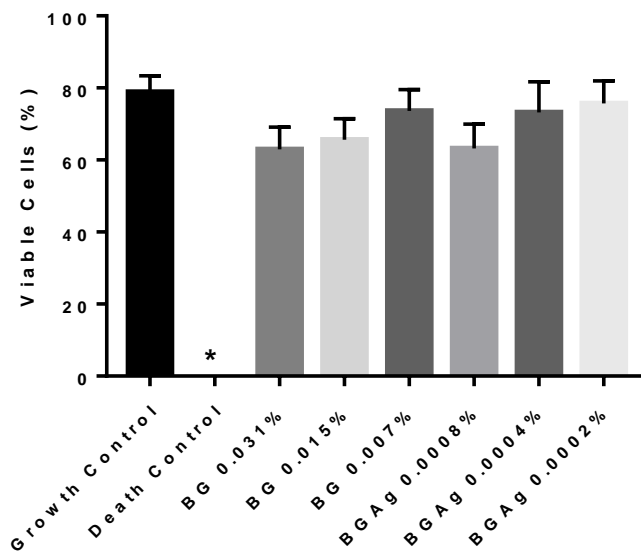


Figure 8. PMN viability in presence of BG (A-L) and BGAg (M-Z). Demonstrative images of Live/Dead™ assay captured by 40x objective (1). The bright field shows cell morphology, GFP shows live cells green stained by calcein, and RFP shows dead cells stained by ethidium homodimer. For growth and death controls, cells were incubated with, respectively, only medium and 80% methanol. (2) Percentage of viable PMNs counted on three aleatory fields. PMNs incubated with different concentrations of BG and BGAg have similar number of viable cells compared to growth control. Results expressed as median with 95% CI. (*P<0.05 compared to growth control).

Silver can induce inflammation, cell activation oxidative stress, ROS production, protein inactivation, inhibition of respiratory chain dehydrogenase, alteration of ionic channels, misbalance of cations/anions metabolism, organelle and DNA damage [16,24,25]. The Ag⁺ can form complexes with biomolecules causing protein dysfunction and loss of enzyme activity (inactivation, loss of tertiary structure, replacement of cofactors, exchange of structural metals, breakage of disulfide bonds, among others), impaired membrane function caused by the loss of membrane potential and mechanical damage, or interference with nutrient uptake [24]. Taken together, these events lead to cell wall breakdown and cytolysis [25]. Although undesirable effects, silver confers antibacterial properties to materials: dissolution products of silver-doped bioactive glasses inhibited *S. aureus* and *E. coli* growth [10,11].

Oxidative stress. Both samples of BG and BGAg alone were unable to induce intra and extracellular ROS production above baseline parameters (Figure 9). However, the high dilution of neat BG decreased ROS detection when coincubated with opsonised zymosan. This compound activates an oxidative burst by binding itself to complement receptors, leading transduction signal to protein kinase C activation and consequent activation of NADPH-oxidase, the key enzyme of oxidative burst [26]. It suggests that BG dissolution products may interfere at zymosan-receptor complex or have the ability to scavenge free radicals and superoxides.

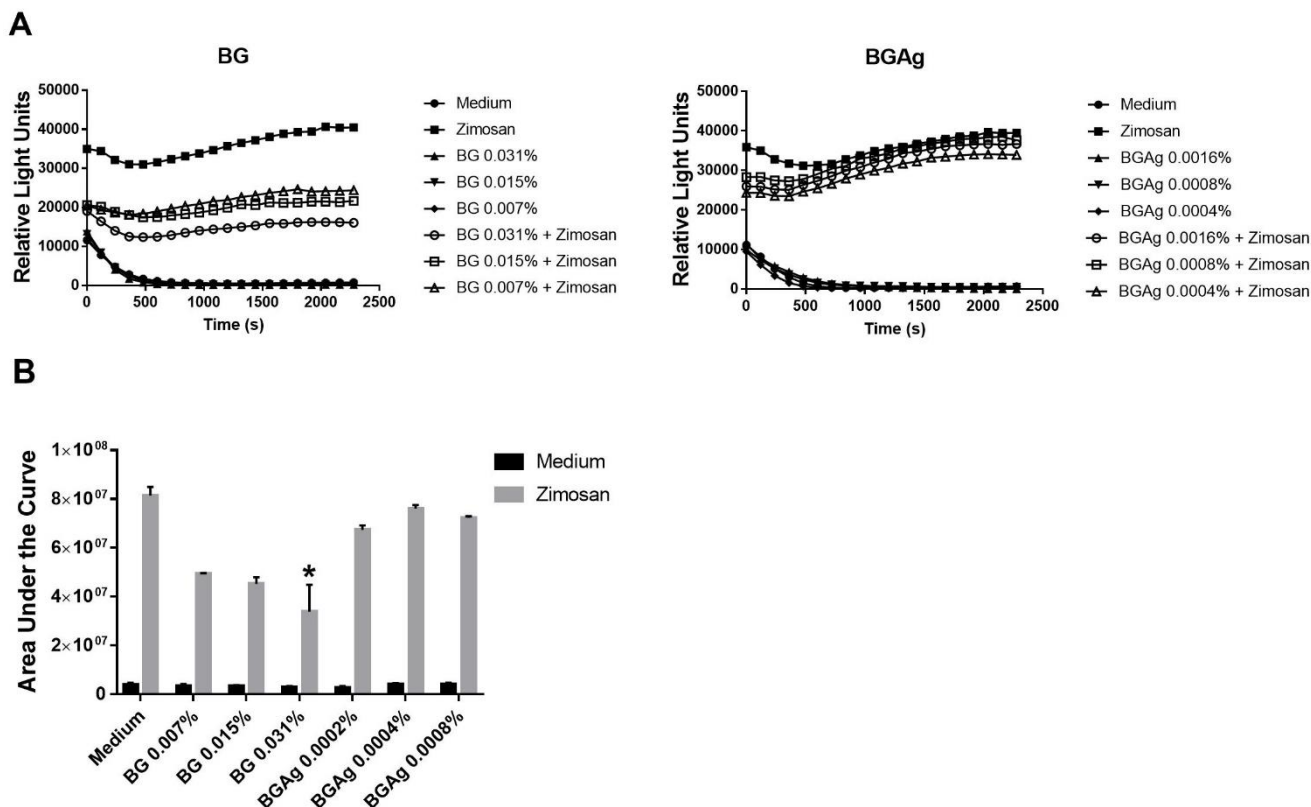


Figure 9. ROS production in PMNs. (A) Chemiluminescent array curves showing similar RLU detection between BG and BGAg samples with negative control (medium only). BG samples decreased ROS production while coincubated with zimosan (positive control). Each bar represents the median of triplicate readings of each *ex vivo* PMN culture (n=3) at the peak of respiratory burst. **(B)** AUC values plotted for each stimulus. The sample BG 0.031% reduced significantly ROS production in comparison with only zimosan stimulus. Values expressed as median with CI. (*P<0.05 compared to positive control).

Cytokine modulation. Quantification of TNF- α , IL-1 β , IL-6, IL-4, and IL-10 at 24h PBMC's culture supernatant performed by sandwich ELISA shown no significant differences between the treatments with three subtoxic BG and BGAg suspensions and baseline control. At some sample concentrations, TNF- α , IL-1 β and IL-10 release was lower than detection limits of the method. These results suggest that bioactive glasses particles even with doped silver do not disturb the basal cytokine levels or acts as synergistic with PHA in PBMC cultures.

The presence of PHA upregulated TNF- α , IL-1 β , IL-6, and IL-10 secretion in contrast with basal. Although, no significant cytokine release by bioactive glass particles with PHA exposure was observed in comparison to PHA treatment alone. Consequently, glasses were inept to modulate the related cytokines release at mimetic inflammatory environment neither.

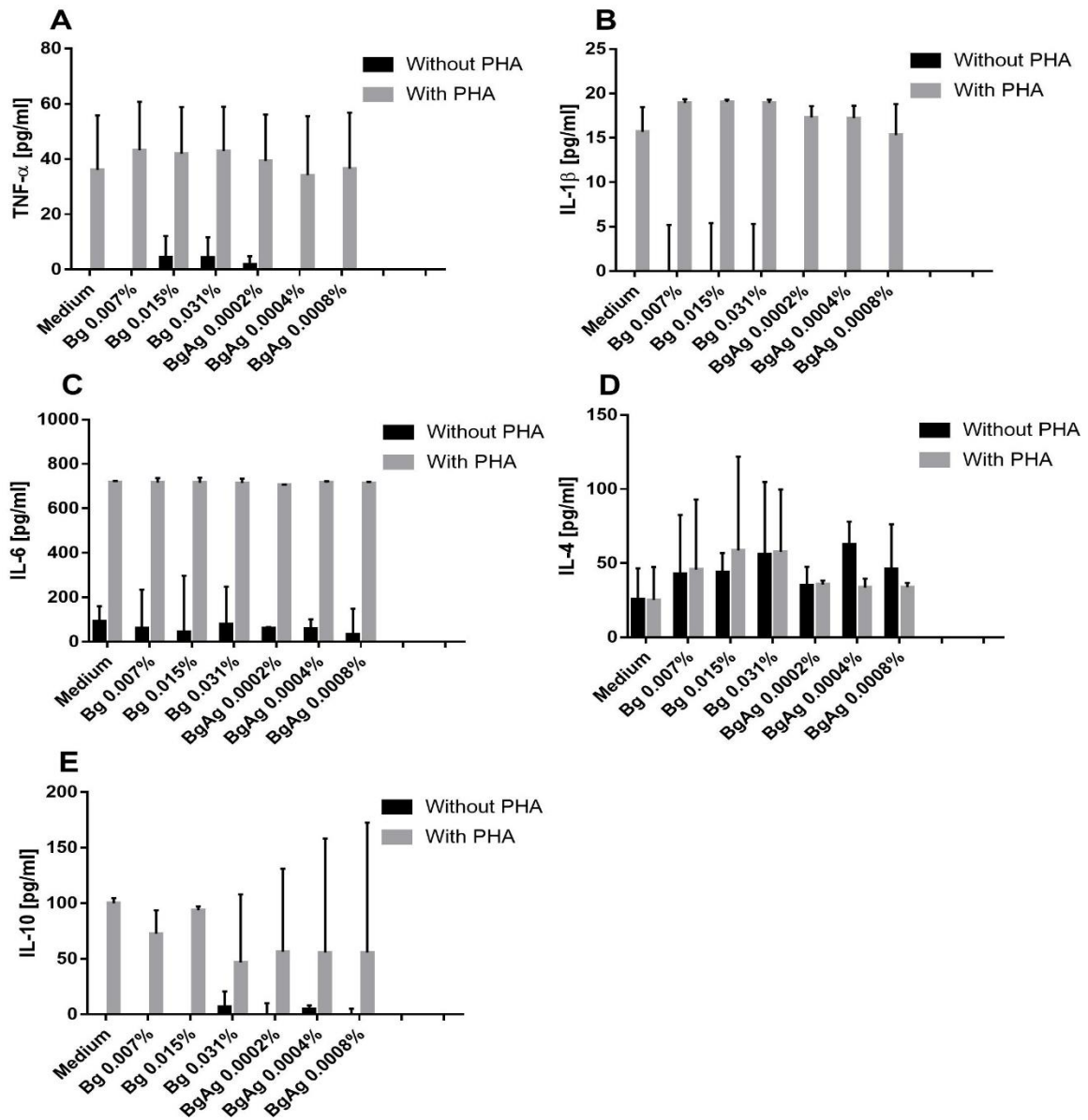


Figure 10. Cytokine release by PBMC cultures incubated with BG and BGAg. Titration of TNF- α (A), IL-1 β (B), IL-6 (C), IL-4 (D) and IL-10 (E) released at 24 hours culture supernatant of PBMC's cultured with or without 5 μ g/ml PHA. There were no significant differences on cytokine's production between BG and BGAg and only medium stimulus. Moreover, bioactive glasses were unable to reduce cytokine levels with PHA coincubation. Data were presented as the median \pm 95% CI of triplicates of each volunteer (n=3).

Immunomodulatory effects of bioactive glasses were investigated by previous studies. Particles belonging to system 60S did not change significantly IL-4 secretion profile by PBMCs [27]. Other study found that 45S5 glass do not interfere at IL-6, IL-10, and TNF- α secretion by non-stimulated macrophages and monocytes cultures falling in agreement with current results [7]. The same study

observed decrease of TNF- α production when the cells were coincubated with LPS. However, 45S5 powders upregulated TNF- α secretion by peritoneal macrophages [28]. Beyond cell population variances, differences on cytokine modulation may be explained by different factors that leads immune response by biomaterials, including composition, size, surface chemistry, plasma protein binding, and exposure route [29].

In some therapies against cancer, arthritis and allergies, immunomodulation is highly desirable. However, immunosuppression or immunostimulation of biomaterials are seen as adverse effects in most of treatments. Thus, the interaction of biomaterials with the immune system is key for the safe medicinal uses. A recent work questioned the current capacity to examine the real function of biomaterials within both innate and adaptive immune responses, mainly concerning to B cell and T cell responses [30]. Although acute and long-term immune toxicities have been developed, studies of treatment and prediction of immunomodulation are scarce [29,30]. Such studies contribute to approach materials science and biomedical engineering application [31].

Conclusions. Silver doped bioactive glasses were successfully prepared using sol-gel method. Topographical analysis revealed highly porous and irregular glass microparticles. The presence of silver increased the glass cytotoxicity against human PBMCs. The BG and BGAg subtoxic concentrations did not play a role at TNF- α , IL-1 β , IL-6, IL-4 and IL-10 modulation. Both BG and BGAg were unable to induce ROS production, while neat BG decreased ROS production when coincubated with serum-opsonised zymosan, suggesting a potential scavenger activity. Further studies of silver dissolution in the used medium and the development of mechanisms for ion release control according to desirable dose are necessary. In this study, we propose simple assays for acute cytotoxicity and cytokine modulation as initial screening for futures trials involving BG or BGAg samples.

Currently, the immune response modulation is considered relevant in regenerative therapies. Biomaterials can modify the adaptive immunity (cell phenotype and cytokine release) to induce tissue repair after tissue injury [32]. The results of present study do not demonstrate an anti-inflammatory/regulatory cytokine profile

induced by BG or BGAg suspensions. Conversely, pro-inflammatory cytokines released were not promoted by glasses suspensions, even with doped silver.

References.

1. Shirliff V, Hench L (2003) Bioactive materials for tissue engineering, regeneration and repair. *Journal of materials science* 38: 4697-4707.
2. Hench LL, Splinter RJ, Allen W, Greenlee T (1971) Bonding mechanisms at the interface of ceramic prosthetic materials. *Journal of Biomedical Materials Research* 5: 117-141.
3. Jones JR, Ehrenfried LM, Hench LL (2006) Optimising bioactive glass scaffolds for bone tissue engineering. *Biomaterials* 27: 964-973.
4. Chouzouri G, Xanthos M (2007) In vitro bioactivity and degradation of polycaprolactone composites containing silicate fillers. *Acta biomaterialia* 3: 745-756.
5. Al-Noaman A, Rawlinson SC, Hill RG (2013) Bioactive glass-stoichiometric wollastonite glass alloys to reduce TEC of bioactive glass coatings for dental implants. *Materials Letters* 94: 69-71.
6. Al-Noaman A, Karpukhina N, Rawlinson SC, Hill RG (2013) Effect of FA addition on bioactivity of bioactive glass coating for titanium dental implant: Part II—Composite coating. *Journal of Non-Crystalline Solids* 364: 99-106.
7. Day RM, Boccaccini AR, Shurey S, Roether JA, Forbes A, et al. (2004) Assessment of polyglycolic acid mesh and bioactive glass for soft-tissue engineering scaffolds. *Biomaterials* 25: 5857-5866.
8. Lin C, Mao C, Zhang J, Li Y, Chen X (2012) Healing effect of bioactive glass ointment on full-thickness skin wounds. *Biomedical Materials* 7: 045017.
9. Hench LL, Jones JR (2015) Bioactive Glasses: Frontiers and Challenges. *Frontiers in bioengineering and biotechnology* 3.
10. Balamurugan A, Balossier G, Laurent-Maquin D, Pina S, Rebelo A, et al. (2008) An in vitro biological and anti-bacterial study on a sol-gel derived silver-incorporated bioglass system. *dental materials* 24: 1343-1351.
11. Zhu H, Hu C, Zhang F, Feng X, Li J, et al. (2014) Preparation and antibacterial property of silver-containing mesoporous 58S bioactive glass. *Materials Science and Engineering: C* 42: 22-30.
12. Baghbani F, Moztafzadeh F, Mozafari M, Raz M, Rezvani H (2016) Production and Characterization of a Ag-and Zn-Doped Glass-Ceramic Material and In Vitro Evaluation of Its Biological Effects. *Journal of Materials Engineering and Performance* 25: 3398-3408.
13. El-Kady AM, Ali AF, Rizk RA, Ahmed MM (2012) Synthesis, characterization and microbiological response of silver doped bioactive glass nanoparticles. *Ceramics International* 38: 177-188.
14. Abudabbus M, Jevremović I, Janković A, Perić-Grujić A, Matić I, et al. (2016) Biological activity of electrochemically synthesized silver doped polyvinyl alcohol/graphene composite hydrogel discs for biomedical applications. *Composites Part B: Engineering* 104: 26-34.

15. Day RM, Boccaccini AR (2005) Effect of particulate bioactive glasses on human macrophages and monocytes in vitro. *Journal of Biomedical Materials Research Part A* 73: 73-79.
16. Paino IMM, Zucolotto V (2015) Poly (vinyl alcohol)-coated silver nanoparticles: Activation of neutrophils and nanotoxicology effects in human hepatocarcinoma and mononuclear cells. *Environmental toxicology and pharmacology* 39: 614-621.
17. Janetzki S, Britten CM, Kalos M, Levitsky HI, Maecker HT, et al. (2009) "MIATA"—minimal information about T cell assays. *Immunity* 31: 527-528.
18. Castellano LR, Correia Filho D, Argiro L, Dessen H, Prata A, et al. (2009) Th1/Th2 immune responses are associated with active cutaneous leishmaniasis and clinical cure is associated with strong interferon- γ production. *Human immunology* 70: 383-390.
19. Spaepen P, De Boodt S, Aerts J-M, Sloten JV (2011) Digital image processing of live/dead staining. *Mammalian Cell Viability: Methods and Protocols*: 209-230.
20. Vulpoi A, Baia L, Simon S, Simon V (2012) Silver effect on the structure of SiO₂-CaO-P₂O₅ ternary system. *Materials Science and Engineering: C* 32: 178-183.
21. El-Kady AM, Farag MM (2015) Bioactive Glass Nanoparticles as a New Delivery System for Sustained 5-Fluorouracil Release: Characterization and Evaluation of Drug Release Mechanism. *Journal of Nanomaterials* 2015.
22. Kavitha R, Subha B, Shanmugam S, Ravichandran K Synthesis and Invitro Characterisation of Lithium Doped Bioactive Glass through Quick Alkali Sol-Gel Method.
23. Zheng K, Solodovnyk A, Li W, Goudouri OM, Stähli C, et al. (2015) Aging Time and Temperature Effects on the Structure and Bioactivity of Gel-Derived 45S5 Glass-Ceramics. *Journal of the American Ceramic Society* 98: 30-38.
24. Lemire JA, Harrison JJ, Turner RJ (2013) Antimicrobial activity of metals: mechanisms, molecular targets and applications. *Nature Reviews Microbiology* 11: 371-384.
25. Hsueh Y-H, Lin K-S, Ke W-J, Hsieh C-T, Chiang C-L, et al. (2015) The antimicrobial properties of silver nanoparticles in *Bacillus subtilis* are mediated by released Ag⁺ ions. *PloS one* 10: e0144306.
26. Sergeant S, McPhail LC (1997) Opsonized zymosan stimulates the redistribution of protein kinase C isoforms in human neutrophils. *The Journal of Immunology* 159: 2877-2885.
27. Silva C, Bozzi A, Pereira M, Goes A, Leite MF. Effects of Bioactive Glass 60S and Biphasic Calcium Phosphate on Human Peripheral Blood Mononuclear Cells; 2004. *Trans Tech Publ.* pp. 841-844.
28. Bosetti M, Hench L, Cannas M (2002) Interaction of bioactive glasses with peritoneal macrophages and monocytes in vitro. *Journal of biomedical materials research* 60: 79-85.

29. Jiao Q, Li L, Mu Q, Zhang Q (2014) Immunomodulation of nanoparticles in nanomedicine applications. *BioMed research international* 2014.
30. Vishwakarma A, Bhise NS, Evangelista MB, Rouwkema J, Dokmeci MR, et al. (2016) Engineering Immunomodulatory Biomaterials To Tune the Inflammatory Response. *Trends in biotechnology* 34: 470-482.
31. Badylak SF (2016) A scaffold immune microenvironment. *Science* 352: 298-298.
32. Sadtler K, Estrellas K, Allen BW, Wolf MT, Fan H, et al. (2016) Developing a pro-regenerative biomaterial scaffold microenvironment requires T helper 2 cells. *Science* 352: 366-370.

3. CONSIDERAÇÕES GERAIS

A primeira etapa deste trabalho consistiu na síntese das amostras de vidro bioativo e vidro bioativo dopado com Ag^{2+} pelo método sol-gel, seguido pela caracterização do material pelas técnicas: microscopia eletrônica de varredura, análise térmica diferencial, análise termal gravimétrica, difração de raio-x, espectroscopia Raman amplificada por superfície e microscopia de força atômica.

A citotoxicidade *in vitro* marcou a segunda etapa do estudo. Para tanto, foi utilizado um protocolo de citotoxicidade aguda em PBMCs humanos baseado na redução da resazurina. As amostras de BG evidenciaram viabilidade significativamente igual ao basal em concentrações superiores a 0,31%, ao contrário do BGA_g que obteve resultado similar com alíquotas de 0,0004%. Esses resultados sugerem cautela na utilização da prata em biomateriais com exposição direta a tecidos vascularizados.

Uma vez determinada a concentração subtóxica dos vidros bioativos, o projeto de pesquisa prosseguiu com avaliação imunomoduladora das amostras, o que consistiu na terceira etapa do estudo. Apesar das amostras BG e BGA_g nas concentrações empregadas não alterarem o perfil de produção das citocinas e ROS mensuradas, tais etapas são cruciais para determinação *in vitro* da resposta imune inata e adaptativa frente ao biomaterial, uma vez em que os componentes utilizados têm potencial para desencadear tais eventos. Essas elucidações são importantes para o aumento da capacidade em identificar, prever e controlar respostas imunológicas a biomateriais implantados. Assim, a observação e o entendimento da imunogênicidade dos vidros bioativos permite o aprimoramento da sua biocompatibilidade em seu mais alto conceito.

Ainda fazem-se necessários estudos para determinação do mecanismo de liberação de prata, bem como os fatores que a modificam. Dessa forma, será possível manipular os vidros bioativos para que a liberação de prata siga um modelo heterogêneo de acordo com a taxa de liberação desejada em determinada terapêutica.

4. CONCLUSÃO

Os vidros bioativos dopados com prata, no presente estudo, foram produzidos com sucesso pelo método sol-gel. As imagens do SEM mostraram partículas micrométricas com superfície irregular e porosa. Os padrões de XRD das amostras investigadas mostraram cristalização incipiente do fosfato tricálcico (TCP). Este resultado sugere que a incorporação de prata para as amostras investigadas não comprometeu a sua bioatividade. Nas curvas do RAMAN-SERS, foi observada a presença de grupos Si-O-Si em todas as amostras, o que demonstra a conservação da estrutura do vidro, mesmo com a adição de prata. No que se refere à citotoxicidade contra PBMCs, o BGAg evidenciou maior citotoxicidade, quando comparado ao BG. As doses subtóxicas em PBMCs não influenciaram significativamente a viabilidade dos PMNs. As amostras de vidro bioativo influenciaram na liberação das citocinas estudadas. Ainda se faz necessário a análise do comportamento de liberação de prata e o desenvolvimento de mecanismos de liberação de íons conforme a dose necessária.

5. REFERÊNCIAS*

1. Hench LL, Splinter RJ, Allen W, Greenlee T (1971) Bonding mechanisms at the interface of ceramic prosthetic materials. *Journal of Biomedical Materials Research* 5: 117-141.
2. Shirliff V, Hench L (2003) Bioactive materials for tissue engineering, regeneration and repair. *Journal of materials science* 38: 4697-4707.
3. Hench LL, West JK (1990) The sol-gel process. *Chemical Reviews* 90: 33-72.
4. Jones JR, Ehrenfried LM, Hench LL (2006) Optimising bioactive glass scaffolds for bone tissue engineering. *Biomaterials* 27: 964-973.
5. Goh YF, Alshemary AZ, Akram M, Kadir A, Rafiq M, et al. (2014) Bioactive Glass: An In-Vitro Comparative Study of Doping with Nanoscale Copper and Silver Particles. *International Journal of Applied Glass Science* 5: 255-266.
6. Al-Noaman A, Karpukhina N, Rawlinson SC, Hill RG (2013) Effect of FA addition on bioactivity of bioactive glass coating for titanium dental implant: Part II—Composite coating. *Journal of Non-Crystalline Solids* 364: 99-106.
7. Al-Noaman A, Karpukhina N, Rawlinson SC, Hill RG (2013) Effect of FA on bioactivity of bioactive glass coating for titanium dental implant. Part I: Composite powder. *Journal of Non-Crystalline Solids* 364: 92-98.
8. Ostomel TA, Shi Q, Tsung CK, Liang H, Stucky GD (2006) Spherical bioactive glass with enhanced rates of hydroxyapatite deposition and hemostatic activity. *Small* 2: 1261-1265.
9. Handel M, Hammer TR, Noeaid P, Boccaccini AR, Hofer D (2013) 45S5-Bioglass®-Based 3D-Scaffolds Seeded with Human Adipose Tissue-Derived Stem Cells Induce In Vivo Vascularization in the CAM Angiogenesis Assay. *Tissue Engineering Part A* 19: 2703-2712.
10. Lim DH, Jang J, Kim S, Kang T, Lee K, et al. (2012) The effects of sub-lethal concentrations of silver nanoparticles on inflammatory and stress genes in human macrophages using cDNA microarray analysis. *Biomaterials* 33: 4690-4699.

11. Hench LL, Jones JR (2015) Bioactive Glasses: Frontiers and Challenges. *Frontiers in bioengineering and biotechnology* 3.
12. Day RM, Maquet V, Boccaccini AR, Jérôme R, Forbes A (2005) In vitro and in vivo analysis of macroporous biodegradable poly (D, L-lactide-co-glycolide) scaffolds containing bioactive glass. *Journal of Biomedical Materials Research Part A* 75: 778-787.
13. Zhu H, Hu C, Zhang F, Feng X, Li J, et al. (2014) Preparation and antibacterial property of silver-containing mesoporous 58S bioactive glass. *Materials Science and Engineering: C* 42: 22-30.
14. Balamurugan A, Balossier G, Laurent-Maquin D, Pina S, Rebelo A, et al. (2008) An in vitro biological and anti-bacterial study on a sol-gel derived silver-incorporated bioglass system. *dental materials* 24: 1343-1351.
15. Baiocco P, Ilari A, Ceci P, Orsini S, Gramiccia M, et al. (2010) Inhibitory effect of silver nanoparticles on trypanothione reductase activity and *Leishmania infantum* proliferation. *ACS medicinal chemistry letters* 2: 230-233.
16. Holt KB, Bard AJ (2005) Interaction of silver (I) ions with the respiratory chain of *Escherichia coli*: an electrochemical and scanning electrochemical microscopy study of the antimicrobial mechanism of micromolar Ag⁺. *Biochemistry* 44: 13214-13223.
17. Labbaf S, Tsigkou O, Müller KH, Stevens MM, Porter AE, et al. (2011) Spherical bioactive glass particles and their interaction with human mesenchymal stem cells in vitro. *Biomaterials* 32: 1010-1018.
18. Day RM, Boccaccini AR, Shurey S, Roether JA, Forbes A, et al. (2004) Assessment of polyglycolic acid mesh and bioactive glass for soft-tissue engineering scaffolds. *Biomaterials* 25: 5857-5866.
19. Detsch R, Stoor P, Grünwald A, Roether JA, Lindfors NC, et al. (2014) Increase in VEGF secretion from human fibroblast cells by bioactive glass S53P4 to stimulate angiogenesis in bone. *Journal of biomedical materials research Part A* 102: 4055-4061.

20. Day RM, Boccaccini AR (2005) Effect of particulate bioactive glasses on human macrophages and monocytes in vitro. *Journal of Biomedical Materials Research Part A* 73: 73-79.
21. Lin C, Mao C, Zhang J, Li Y, Chen X (2012) Healing effect of bioactive glass ointment on full-thickness skin wounds. *Biomedical Materials* 7: 045017.
22. Abudabbus M, Jevremović I, Janković A, Perić-Grujić A, Matic I, et al. (2016) Biological activity of electrochemically synthesized silver doped polyvinyl alcohol/graphene composite hydrogel discs for biomedical applications. *Composites Part B: Engineering* 104: 26-34.
23. Paino IMM, Zucolotto V (2015) Poly (vinyl alcohol)-coated silver nanoparticles: Activation of neutrophils and nanotoxicology effects in human hepatocarcinoma and mononuclear cells. *Environmental toxicology and pharmacology* 39: 614-621.
24. Gordon S, Taylor PR (2005) Monocyte and macrophage heterogeneity. *Nature Reviews Immunology* 5(12): 953-964.
25. El-Kady AM, Ali AF, Rizk RA, Ahmed MM (2012) Synthesis, characterization and microbiological response of silver doped bioactive glass nanoparticles. *Ceramics International* 38: 177-188.

* De acordo com as normas do PPGO/UFPB, baseadas na norma do International Committee of Medical Journal Editors - Grupo de Vancouver. Abreviatura dos periódicos em conformidade com o Medline.